Supplemental Information

Supplemental Data

- **Figure S1 related to Figures 2, and 3**
- **Figure S2 related to Figure 2F**
- **Figures S3 and S4 related to Figure 2G**
- **Figure S5 related to Figure 3**
- **Figure S6 related to Figure 4**
- **Figure S7 related to Figures 5 and 6**

Figure S1

A. mouse osteocalcin antibody

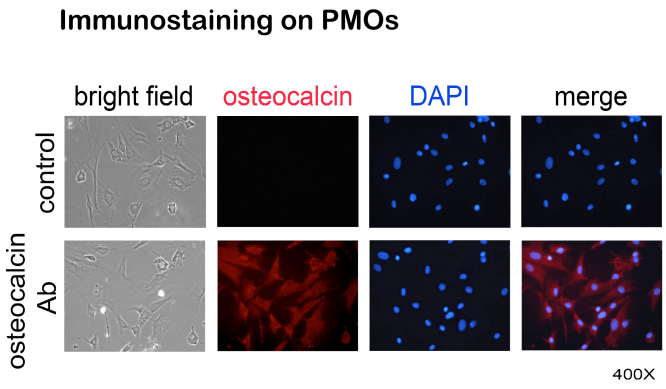

B. Tie2 antibody

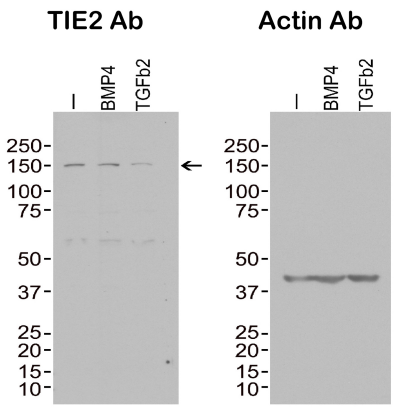

C. human osteocalcin antibody (OCG4)

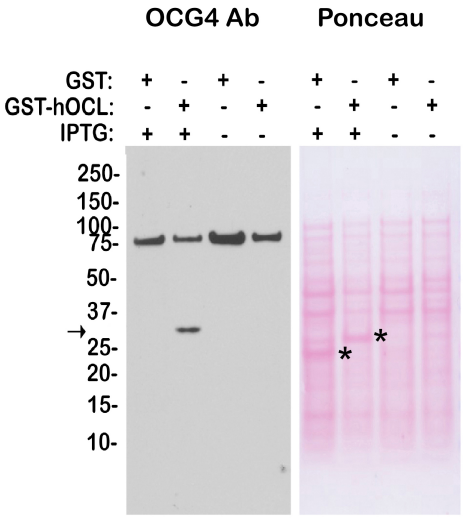

D. anti-human BMP4 antibody

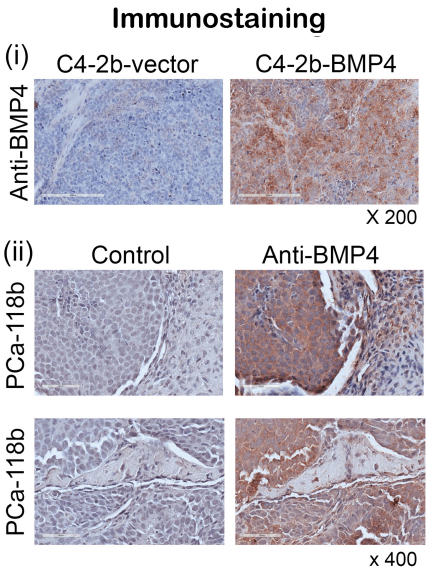

E. anti-human TGFβ2 antibody

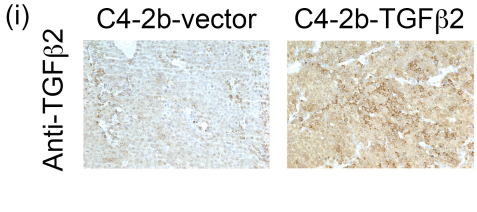

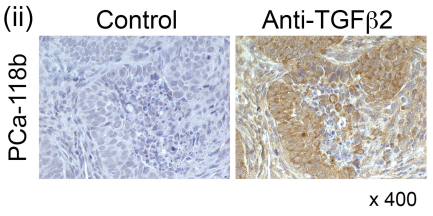

Figure S1, related to Figures 2 and 3. Validation of antibodies used in this study. (A) Validation of mouse osteocalcin antibody. Goat anti-mouse osteocalcin antibody (sc-23790) was purchased from Santa Cruz Biotech. The immunogen was a peptide from an internal region of mouse osteocalcin and the antibody was generated in goats. The antiserum was predicted to react with mouse osteocalcin but not human osteocalcin. PMOs were isolated from neonatal mouse calvariae, and cultured to confluence in alpha MEM containing 10% FBS. The cells attached on the coverslips were washed with PBS, fixed in cold methanol, and dried. Immunofluorescence staining using goat anti-mouse osteocalcin antibody at 1:100 dilution on primary mouse osteoblasts (PMOs) was performed. Immunostaining in the absence of primary antibody was used as a control. (B) Validation of Tie2 antibody. Rabbit anti-Tie2 antibody (sc-9026) was purchased from Santa Cruz Biotech. Western blot using the cell lysates prepared from 2H11 endothelial cells treated with or without BMP4 or TGFb2 showed the Tie2 antibody recognized a protein with apparent molecular mass of 140 kDa, which is the predicted size of Tie2. (C) Validation of human osteocalcin antibody (OCG4). Anti-human osteocalcin antibody (OCG4) was purchased from Takara Bio Inc. (M044) and is a mouse monoclonal antibody. The immunogen is bovine osteocalcin. The antibody can recognize human osteocalcin but not mouse osteocalcin. cDNA encoding human osteocalcin was obtained by RT-PCR using RNA prepared from PC3 cells. The human osteocalcin cDNA was inserted into pGEX-4T vector. GST fusion protein containing human osteocalcin was generated and used to test the reactivity of OCG4. Asterisk (*) indicates the GST protein and GST-human osteocalcin fusion protein (GST-hOCL) induced by IPTG. (D) Validation of anti-human BMP2/4 antibody. Biotinylated anti-human BMP2/4 antibody was purchased from R&D Systems (BAF355) and is a goat polyclonal antibody. (i) Immunohistochemistry of tumors generated from C4-2b-vector versus C4-2b-BMP4 cells. (ii) Immunohistochemistry of PCa-118b tumors. (E) Validation of rabbit anti-TGFβ2 antibody (Proteintech #19999-1-AP). (i) Immunohistochemistry of tumors derived from C4-2b-vector vs. C4-2b-TGFβ2 cells. (ii) Immunohistochemistry of TGFβ2 expression in PCa-118b tumor. Immunostaining in the absence of primary antibody was used as a control.

Figure S2

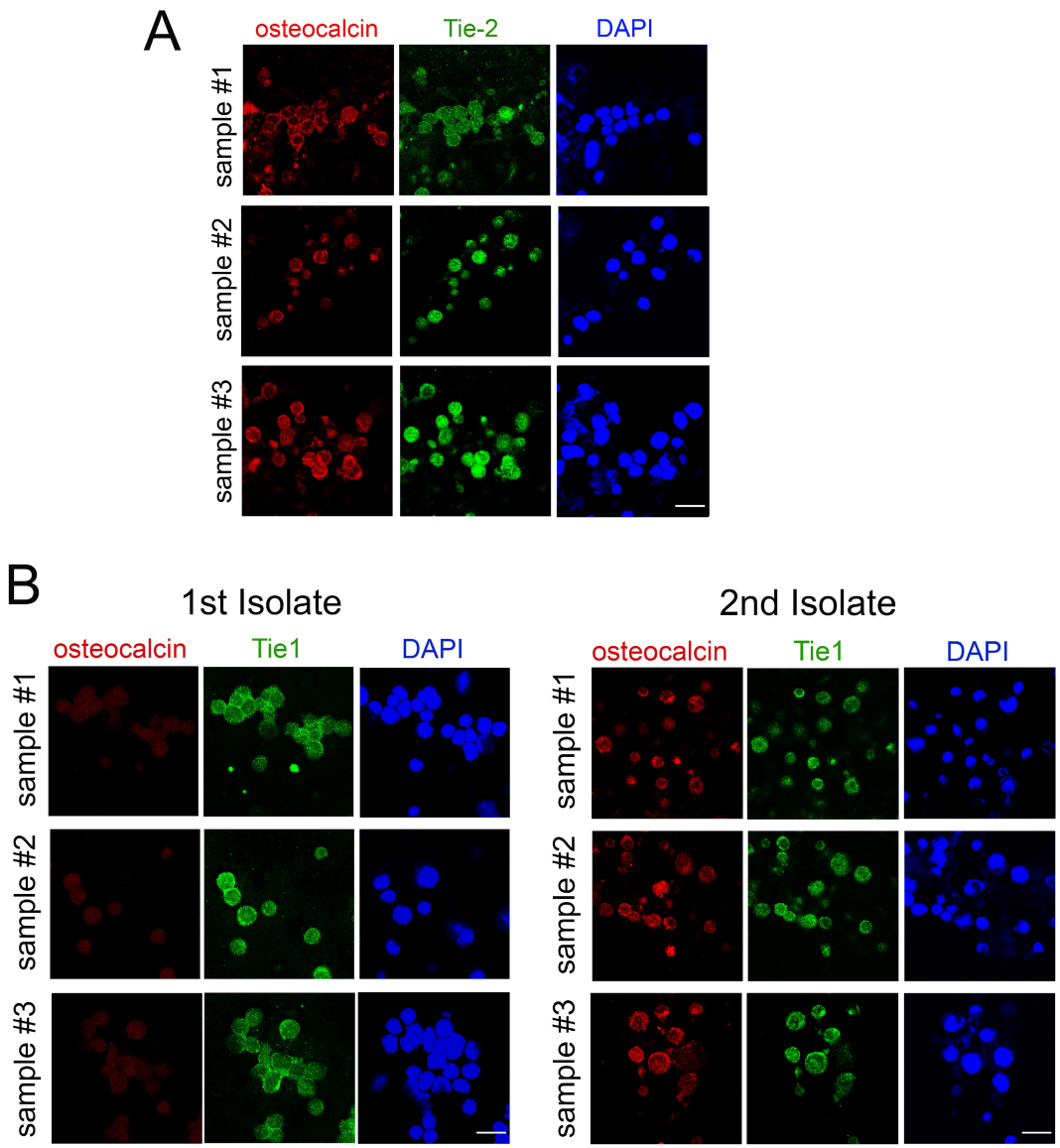

Figure S2, related to Figure 2F. (A) Expression of Tie2 and osteocalcin in cells present in 2nd isolate from three PCa-118b tumors (samples #1-3). Cells from 2nd isolate were directly spotted on cover slips and allowed to dry. Cells were then immunostained with anti-osteocalcin (red fluorescence) and anti-Tie2 (green fluorescence) antibodies. The cell nuclei were stained with DAPI. (B) Expression of Tie1 and osteocalcin in cells prepared from the 1st and 2nd isolate from three PCa-118b tumors (samples #1-3). Cells from 2nd isolate were directly spotted on cover slips and allowed to dry. The cells were immunostained with antibodies against Tie-1 and osteocalcin. Tie-1 positive cells are present in both 1st and 2nd isolate. Only cells in 2nd cell isolate co-express osteocalcin and Tie-1. The cell nuclei were stained with DAPI. Confocal images were taken on an Olympus FV1000 microscope. Scale bars, 20 µm.

Figure S3

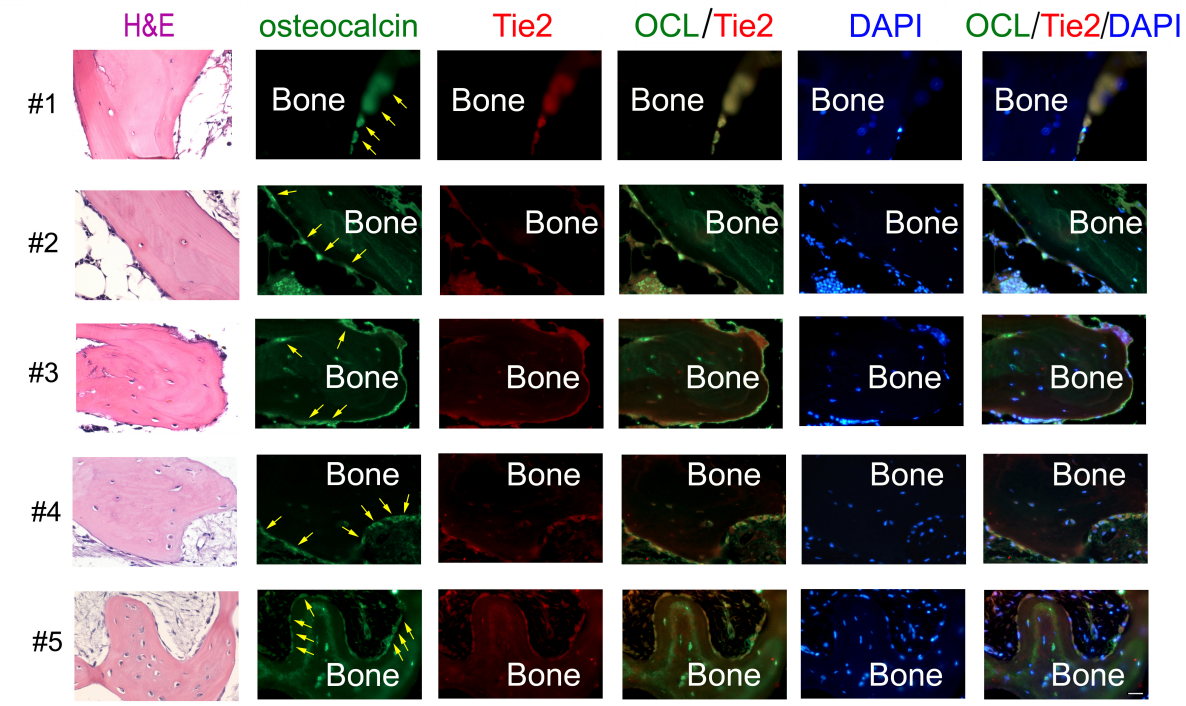

Figure S3, related to Figure 2G. Co-staining of osteocalcin (OCL) and Tie2 in five human PCa bone metastasis specimens. Arrows point to osteocalcin and Tie2 double-positive cells lining the bone. Images were taken on an Olympus IX71 microscope. Scale bar, 25 μm.

Figure S4

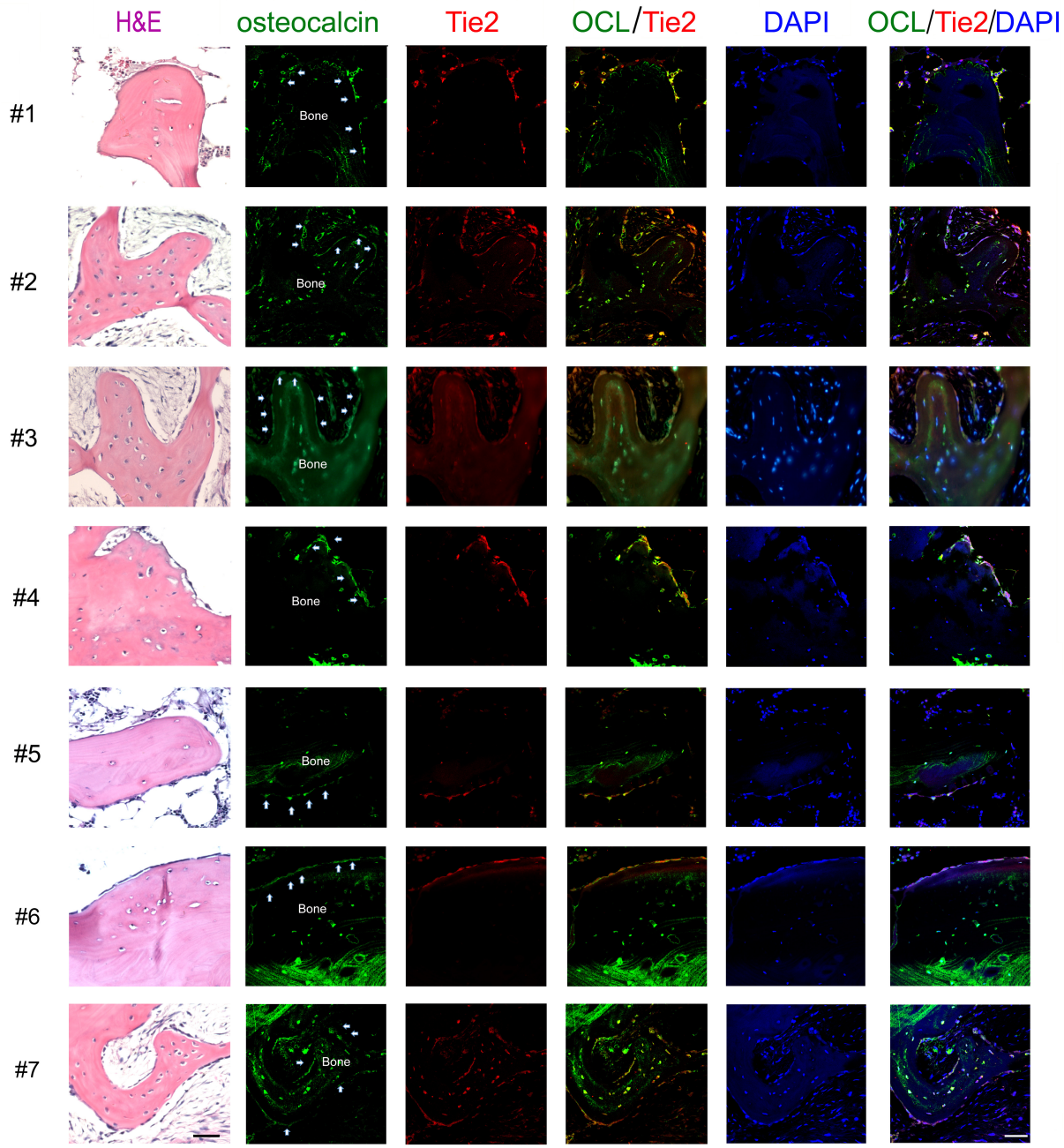

Figure S4, related to Figure 2G. Confocal images of co-staining of osteocalcin (OCL) and Tie2 in seven human PCa bone metastasis specimens. Arrows point to osteocalcin and Tie2 double-positive cells lining the bone. Confocal images were taken on an Olympus FV1000 microscope. Scale bar, 25 μm.

Figure S5

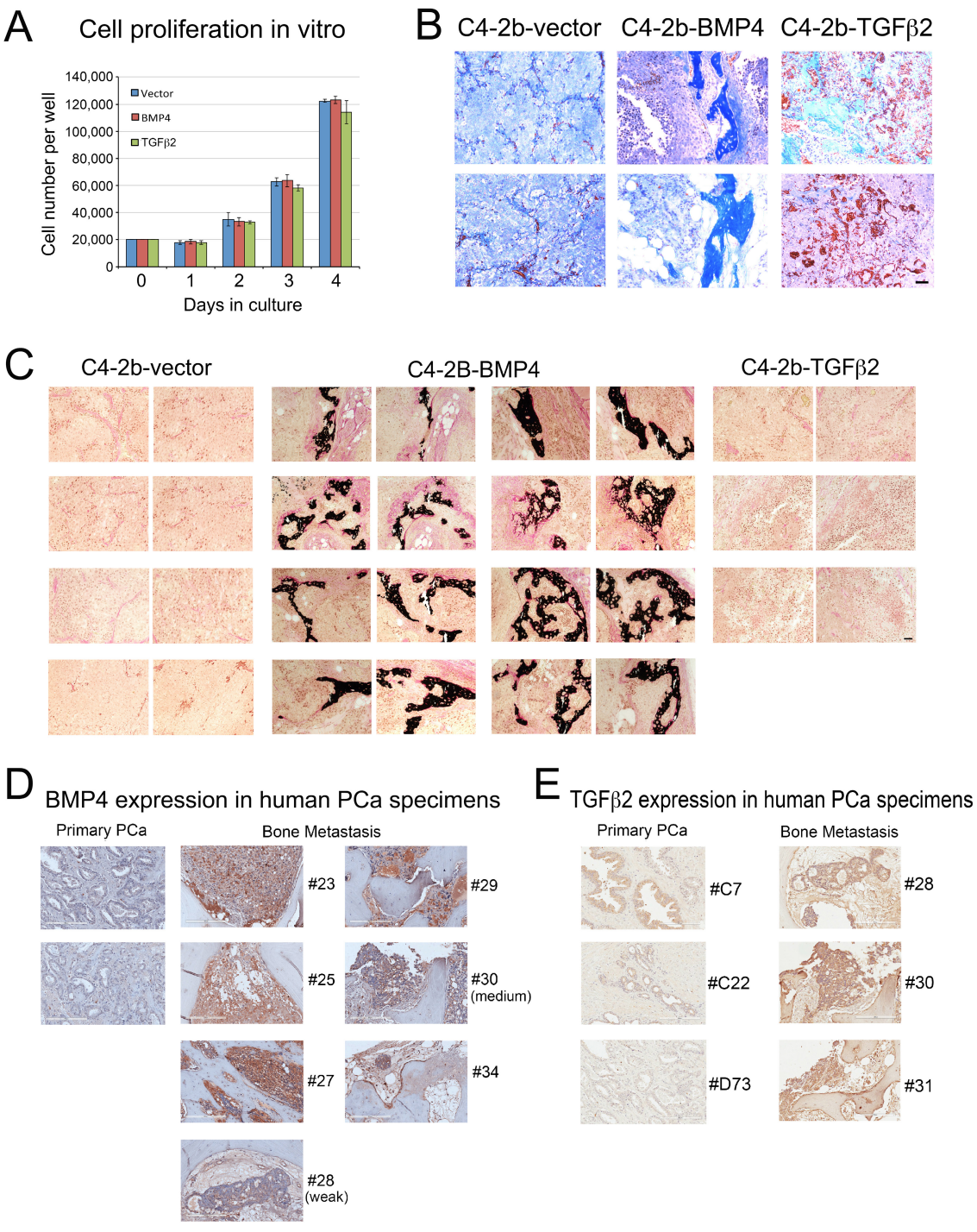
A
Cell proliferation in vitro
Cell number per well
140,000
120,000
100,000
80,000
60,000
40,000
20,000
0
Vector
BMP4
TGFβ2
0
1
2
3
4
Days in culture
B
C4-2b-vector
C4-2b-BMP4
C4-2b-TGFβ2
C
C4-2b-vector
C4-2B-BMP4
C4-2b-TGFβ2
D
BMP4 expression in human PCa specimens
Primary PCa
Bone Metastasis
#23
#29
#25
#30
(medium)
#27
#34
#28
(weak)
E
TGFβ2 expression in human PCa specimens
Primary PCa
Bone Metastasis
#C7
#28
#C22
#30
#D73
#31

Figure S5, related to Figure 3. (A) Effects of overexpression of BMP4 and TGFβ2 on C4-2b cell proliferation in vitro. Overexpression of BMP4 or TGFβ2 in C4-2b cells did not have a significant effect on cell proliferation in vitro. (B) Histological analyses of C4-2b-vector, C4-2b-BMP4, and C4-2b-TGFβ2 tumors by Goldner's Trichrome staining. The C4-2b-BMP4-induced ectopic bone was located close to the edge of the tumor. The C4-2b-TGFβ2 tumors contained abundant extracellular matrices that did not stain with Goldner's Trichrome stain, suggesting that the matrix was not mineralized. Images were taken on an Olympus IX71 microscope. Scale bar, 50 μm. (C) von Kossa staining of C4-2b-vector, C4-2b-BMP4, and C4-2b-TGFβ2 tumors. Images were taken on an Olympus IX71 microscope. Scale bar, 50 μm. (D) Expression of BMP4 in human prostate cancer specimens. Immunohistochemistry of BMP4 in paraffin-embedded human prostate cancer specimens. Two samples from primary tumors and seven samples from bone metastasis are shown. Aperio ImageScope images, scale bar, 200 μm. (E) Expression of TGFβ2 in human prostate cancer specimens. Immunohistochemistry of TGFβ2 in paraffin-embedded human prostate cancer specimens. Three samples from primary tumors and three samples from bone metastasis are shown. Aperio ImageScope images, scale bar, 200 μm.

Supplemental Figure S6

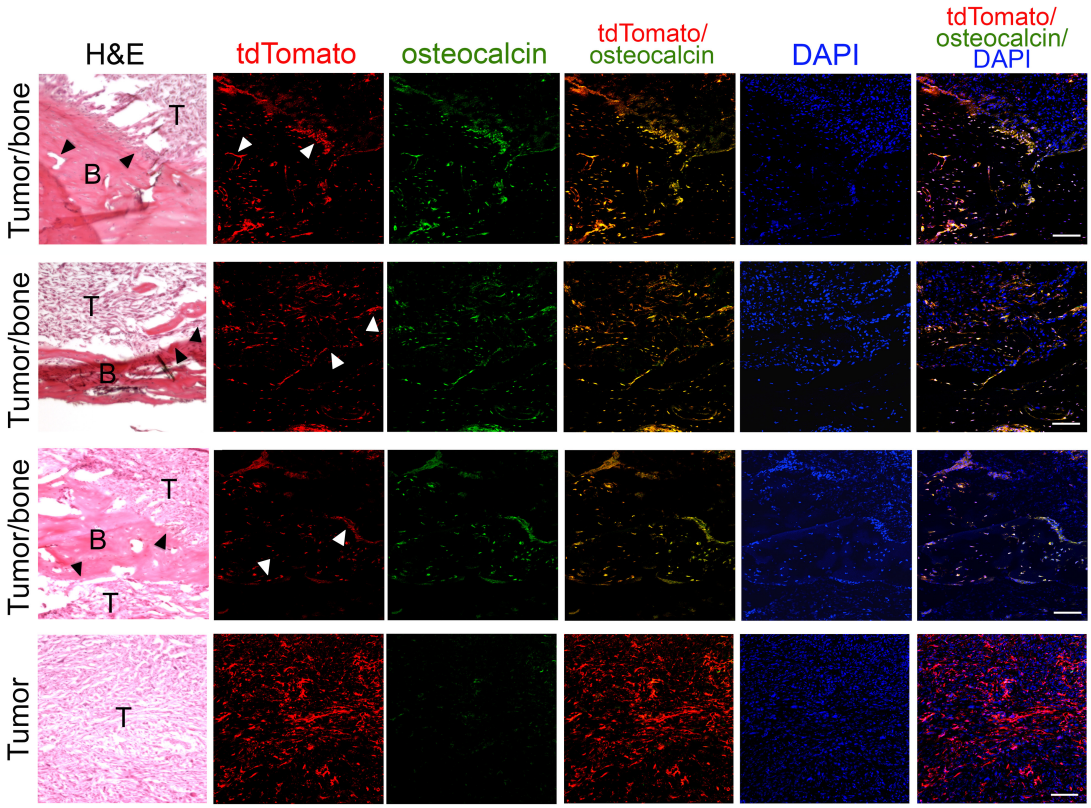

Figure S6, related to Figure 4. Co-expression of osteocalcin with Tie2 in tumor-induced osteoblasts in $Tie2^{Cre}/Rosa^{tdTomato}$ mouse. TRAMP-BMP4 cells were injected into right femur of $Tie2^{Cre}/Rosa^{tdTomato}$ mice for seven weeks. Femurs were collected for histological analyses. Frozen sections of femurs were immunostained for osteocalcin. Confocal images of co-staining of osteocalcin (OCL) and Tie2 (tdTomato) are shown. Arrowheads point to the tumor-induced osteoblasts. Confocal images were taken on an Olympus FV1000 microscope. Scale bars are at 50 μm. B, bone; T, tumor.

Figure S7

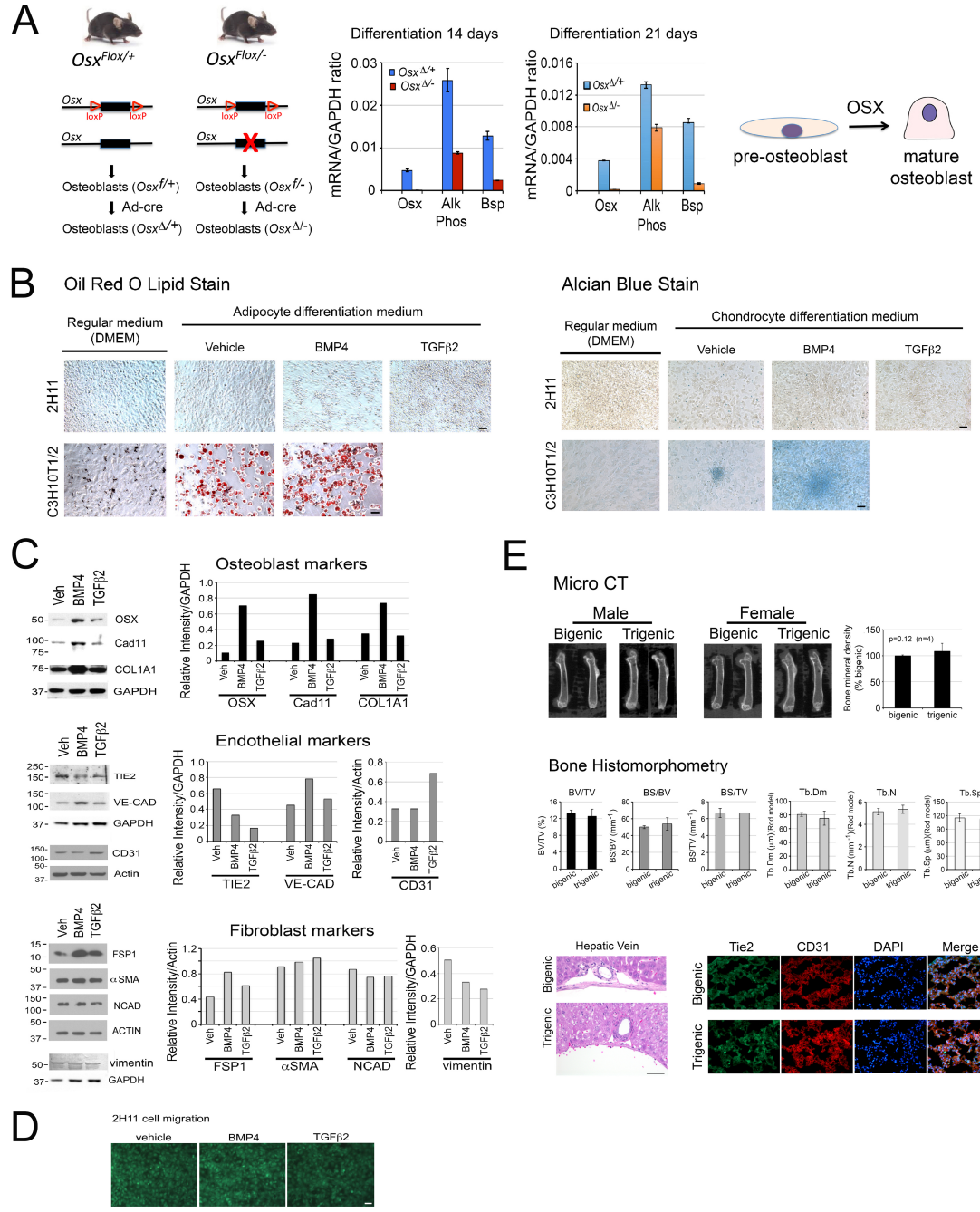
A
Osx^Flox/+
Osx^Flox/-
Osx
loxP
Osteoblasts (Osx f/+)
Ad-cre
Osteoblasts (Osx Δ/+)
Osteoblasts (Osx f/-)
Osteoblasts (Osx Δ/-)
Differentiation 14 days
Differentiation 21 days
mRNA/GAPDH ratio
Osx Δ/+
Osx Δ/-
Osx
Alk Phos
Bsp
pre-osteoblast
OSX
mature osteoblast
B
Oil Red O Lipid Stain
Regular medium (DMEM)
Adipocyte differentiation medium
Vehicle
BMP4
TGFβ2
2H11
C3H10T1/2
Alcian Blue Stain
Chondrocyte differentiation medium
C
Osteoblast markers
Relative Intensity/GAPDH
OSX
Cad11
COL1A1
GAPDH
Endothelial markers
TIE2
VE-CAD
CD31
Actin
Fibroblast markers
FSP1
αSMA
NCAD
ACTIN
vimentin
Relative Intensity/Actin
D
2H11 cell migration
vehicle
BMP4
TGFβ2
E
Micro CT
Male
Female
Bigenic
Trigenic
Bone mineral density (% bigenic)
p=0.12 (n=4)
Bone Histomorphometry
BV/TV
BS/BV
BS/TV
Tb.Dm
Tb.N
Tb.Sp
Hepatic Vein
Tie2
CD31
DAPI
Merge

Figure S7 related to Figure 5. (A) Knockout of *Osx* in calvarial osteoblasts inhibits osteoblast maturation. Left, calvarial osteoblasts isolated from mice with $Osx^{flox/+}$ and $Osx^{flox/-}$ genotype were infected with adenoviral vector containing *cre* to delete the floxed *osx* allele. Middle panels, osteoblasts were cultured in differentiation medium for indicated times. RNAs were prepared and the message levels for *Osx*, alkaline phosphatase, and bone sialoprotein (BSP) were determined by qRT-PCR. Right panel, diagram illustrating that OSX is required for osteoblast maturation. (B) 2H11 cells cannot differentiation into adipocytes or chondrocytes. Left panel, 2H11 cells were treated with 100 ng/ml of BMP4 or 20 ng/ml of TGFβ2 for 13 days in adipocyte differentiation medium followed by Oil Red O staining for 30 min at room temperature. C3H10T1/2 cells treated with BMP4 (50 ng/ml) were cultured and stained similarly. Scale bar, 50 μm. Right panel, 2H11 cells were treated with 100 ng/ml of BMP4 or 20 ng/ml of TGFβ2 for 17 days in chondrocyte differentiation medium followed by Alcian Blue staining for 30 min at room temperature. C3H10T1/2 cells treated with BMP2 (20 ng/ml) were cultured and stained similarly. Images were taken on an Olympus IX71 microscope. Scale bar, 50 μm. (C) Characterization of marker gene expression and migration of 2H11 cells. 2H11 cells were treated with 100 ng/ml of BMP4 or 20 ng/ml of TGFβ2 for 3 days in serum-free medium followed by Western blot or Boyden chamber migration assay (D). (E) Characterization of skeletal and vascular phenotypes of bigenic and trigenic mice. Upper panel, Micro CT analysis of femurs. Middle panel, Bone histomorphometry of femurs. Bottom panel (left), Hepatic vessels of bigenic and trigenic mice. Scale bar at 100 μm. Bottom panel (right), Immunostaining of Tie2 and CD31 in the lung tissues of bigenic and trigenic mice. Images were taken on an Olympus IX71 microscope. Scale bar at 50 μm.